# SOLVING SPLINE COLLOCATION APPROXIMATIONS TO NONLINEAR TWO-POINT BOUNDARY VALUE PROBLEMS BY A HOMOTOPY METHOD

by

Layne T. Watson
Melvin R. Scott

CS84015-R

# SOLVING SPLINE COLLOCATION APPROXIMATIONS TO NONLINEAR TWO-POINT BOUNDARY VALUE PROBLEMS BY A HOMOTOPY METHOD

LAYNE T. WATSON† and MELVIN R. SCOTT‡

**Abstract.** The Chow-Yorke algorithm is a homotopy method that has been proved globally convergent for Brouwer fixed point problems, certain classes of zero finding and nonlinear programming problems, and two-point boundary value approximations based on shooting and finite differences. The method is numerically stable and has been successfully applied to a wide range of practical engineering problems. Here the Chow-Yorke algorithm is proved globally convergent for a class of spline collocation approximations to nonlinear two-point boundary value problems. Several numerical implementations of the algorithm are briefly described, and computational results are presented for a fairly difficult fluid dynamics boundary value problem.

**Key words.** homotopy method, Chow-Yorke algorithm, globally convergent, two-point boundary value problem, spline collocation, nonlinear equations

**1. Introduction.** The foundation of the Chow-Yorke algorithm was laid in 1976, and since that time both the theory and the scope of its practical applicability have been greatly extended. This homotopy algorithm is accurately described as a globally convergent probability one algorithm. It is truly globally convergent in the sense that it will converge to a solution of the problem from an *arbitrary* starting point. The phrase "probability one" refers to the rigorous theoretical results which guarantee convergence for almost all choices of some parameter, i.e., with probability one.

Homotopy methods (both continuous [1] and simplicial [9,23]) were once believed to be hopelessly inefficient, and dismissed by some as inherently inferior to quasi-Newton algorithms. Another prevalent point of view was that homotopy algorithms were just continuation, and nothing new. These beliefs have been somewhat dispelled by a series of problems, successfully solved by homotopy methods, on which continuation and quasi-Newton methods either totally failed or experienced great difficulty [39]. Current implementations of these globally convergent probability one homotopy algorithms are reasonably efficient, and their robustness, stability, and accuracy have never been in doubt. A reasonable attitude toward homotopy methods is that they are a method of last resort, but a very powerful and realistic method of last resort.

There are three distinct, but interrelated, aspects of homotopy methods: 1) construction of the right homotopy map, 2) theoretical proof of global convergence for this homotopy map, and 3) tracking the zero curve of this homotopy map. The first aspect is currently still an art, although this is much better understood now due to the accumulation of computational experience [27-33]. Although much remains to be done, significant progress has been made on the second aspect. Global convergence has been proved for Brouwer fixed point problems[35], certain classes of zero finding[36] and nonlinear programming (both unconstrained and constrained) problems[33], and two-point boundary value approximations based on shooting[37] and finite differences[38]. Recently Morgan [20,21] obtained some elegant results for polynomial systems, and the present work considers spline collocation. Various curve tracking algorithms have been around for a long time (e.g., [5], [13-18], [22]), but there is an important distinction between general curve tracking algorithms and

† Applied Mathematics Division 2646, Sandia National Laboratories, Albuquerque, NM 87185. Current address: Department of Computer Science, Virginia Polytechnic Institute & State University, Blacksburg, VA 24061.

‡ Applied Mathematics Division 2646, Sandia National Laboratories, Albuquerque, NM 87185.

This work was supported by Department of Energy Contract DE-AC04-76DP00789 and NSF Grant MCS 8207217.

homotopy curve tracking algorithms. The object of the former is the zero curve *itself*, whereas the object of the latter is a point at $\lambda = 1$. This difference was emphasized in [35], [34], and [38], and the normal flow tracking algorithm (proposed by Georg [11]) described here is more in the spirit of homotopy methods than a general tracker.

Section 2 outlines the theoretical foundation of globally convergent probability one homotopy methods, and proves some convergence theorems for spline collocation approximations to nonlinear two-point boundary value problems. Section 3 discusses several algorithms for tracking the homotopy curves, as well as some pertinent details of the software package HOMPACK used to obtain the numerical results. Section 4 considers a nontrivial two-point boundary value problem from fluid dynamics, presents numerical results from several different approaches to the problem, and illustrates graphically the dependence of the solution on the problem parameters.

**2. Theory.** Consider the two-point boundary value problem

$$y''(x) = f(x, y(x), y'(x)), \qquad 0 \le x \le 1, \tag{1}$$

$$y(0) = y(1) = 0, \tag{2}$$

where $y(x)$ is an $\hat{n}$-dimensional vector function and $f(x, u, v)$ is an $\hat{n}$-dimensional $C^2$ vector function. More general boundary conditions will be considered later. For the interval $[0, 1]$ choose the mesh points

$$0 = x_0 < x_1 < x_2 < \cdots < x_n < x_{n+1} = 1,$$

where

$$x_1 = \delta, \; x_{n+1} = x_n + \delta, \; 0 < \delta \ll 1,$$

and the spacing could be determined by some adaptive scheme, if necessary. For a positive even integer $k > 2$ (the spline order) choose the knot sequence

$$\tau = \Big(\underbrace{x_0, \ldots, x_0}_{k \text{ times}}, x_{k/2}, x_{k/2+1}, \ldots, x_{n-k/2}, x_{n-k/2+1}, \underbrace{\tilde{x}_{n+1}, \ldots, \tilde{x}_{n+1}}_{k \text{ times}}\Big)$$

where $\tilde{x}_{n+1} = x_{n+1} + \delta$ (choosing the last knot just to the right of $x_{n+1}$ is necessary when using right continuous B-splines, because if $\tilde{x}_{n+1} = x_{n+1}$ all the B-splines would be zero at $x_{n+1}$). Let $B_i(x) = B_{i,k,\tau}(x)$ denote the $i$th B-spline of order $k$ defined on the knot sequence $\tau$ given above. There are $n + 2$ such B-splines, and so the dimension of the spline space with basis $\{B_i\}$ is $n + 2$.

Substituting the approximations

$$y_m(x) \approx A_m(x) = \sum_{i=1}^{n+2} \alpha_{mi} B_i(x), \qquad m = 1, \ldots, \hat{n}, \tag{3}$$

into the equations (1–2) yields the nonlinear system of equations

$$A_m(x_0) = 0, \tag{4}$$

(5) $$-A_m''(x_j) + f_m(x_j, A(x_j), A'(x_j)) = 0, \qquad j = 1, \ldots, n,$$

(6) $$A_m(x_{n+1}) = 0; \qquad m = 1, \ldots, \hat{n}.$$

Let $Y = \left(\alpha_{11}, \alpha_{12}, \ldots, \alpha_{1,n+2}, \alpha_{21}, \ldots, \alpha_{2,n+2}, \ldots, \alpha_{\hat{n}1}, \ldots, \alpha_{\hat{n},n+2}\right)^t$. Then the system of equations (4–6) has the form

(7) $$F(Y) = MY + N(Y) = 0,$$

where

$$M = \begin{pmatrix} \bar{M} & 0 & \ldots & 0 \\ 0 & \bar{M} & \ldots & 0 \\ \vdots & \vdots & \ddots & \vdots \\ 0 & 0 & \ldots & \bar{M} \end{pmatrix},$$

$$\bar{M} = \begin{pmatrix} B_1(x_0) & 0 & 0 & & & \\ -B_1''(x_1) & -B_2''(x_1) & -B_3''(x_1) & & * & \\ -B_1''(x_2) & -B_2''(x_2) & -B_3''(x_2) & & & \\ & & & \ddots & & \\ & & & -B_n''(x_{n-1}) & -B_{n+1}''(x_{n-1}) & -B_{n+2}''(x_{n-1}) \\ & * & & -B_n''(x_n) & -B_{n+1}''(x_n) & -B_{n+2}''(x_n) \\ & & & B_n(x_{n+1}) & B_{n+1}(x_{n+1}) & B_{n+2}(x_{n+1}) \end{pmatrix},$$

$$\begin{aligned} N(Y) = \big(&0, f_1(x_1, A(x_1), A'(x_1)), \ldots, f_1(x_n, A(x_n), A'(x_n)), 0, \\ &0, f_2(x_1, A(x_1), A'(x_1)), \ldots, f_2(x_n, A(x_n), A'(x_n)), 0, \\ &\vdots \\ &0, f_{\hat{n}}(x_1, A(x_1), A'(x_1)), \ldots, f_{\hat{n}}(x_n, A(x_n), A'(x_n)), 0\big). \end{aligned}$$

Thus the two-point boundary value problem (1–2) is approximated by the nonlinear system of equations (7), which has dimension

$$p = \hat{n}(n+2).$$

A homotopy method is used to solve (7).

Because of the concavity of B-splines near their center of support, it is possible to choose the mesh points $x_i$ such that the matrix $\bar{M}$ has positive diagonal elements and nonpositive off-diagonal elements. Henceforth it will be tacitly assumed that the mesh points have been so chosen. Because of the B-spline property

$$\sum_{i=1}^{n+2} B_i(x) = 1, \qquad x_0 < x < \tilde{x}_{n+1},$$

the matrix $\bar{M}$ is also row diagonally dominant. Furthermore, $\bar{M}$ is invertible. (Observe that removing the first row and column from $\bar{M}$ leaves an irreducible row diagonally dominant submatrix, which is invertible [8]. Hence $\det \bar{M} \neq 0$.) An invertible, row diagonally dominant matrix with positive diagonal elements is a P-matrix (all its principal minors are positive) [10]. Therefore $\bar{M}$ and $M$

are P-matrices. Actually, the stronger statement that $M$ is a K-matrix (P-matrix with nonpositive off-diagonal elements[10]) can be made, but this fact will not be needed here.

The following four lemmas from [37],[37],[36],[38] respectively will be useful.

*Lemma 1.* Let $g : E^p \to E^p$ be a $C^2$ map, $a \in E^p$, and define $\rho_a : [0,1) \times E^p \to E^p$ by

$$\rho_a(\lambda, y) = \lambda g(y) + (1-\lambda)(y-a).$$

Then for almost all $a \in E^p$ there is a zero curve $\gamma$ of $\rho_a$ emanating from $(0,a)$ along which the Jacobian matrix $D\rho_a(\lambda, y)$ has full rank.

*Lemma 2.* If the zero curve $\gamma$ in Lemma 1 is bounded, it has an accumulation point $(1, \bar{y})$, where $g(\bar{y}) = 0$. Furthermore, if $Dg(\bar{y})$ is nonsingular, then $\gamma$ has finite arc length.

*Lemma 3.* Let $F : E^p \to E^p$ be a $C^2$ map such that for some $r > 0$, $x\,F(x) \geq 0$ whenever $\|x\| = r$. Then $F$ has a zero in $\{x \in E^p \mid \|x\| \leq r\}$, and for almost all $a \in E^p$, $\|a\| < r$, there is a zero curve $\gamma$ of

$$\rho_a(\lambda, x) = \lambda F(x) + (1-\lambda)(x-a),$$

along which the Jacobian matrix $D\rho_a(\lambda, x)$ has full rank, emanating from $(0,a)$ and reaching a zero $\bar{x}$ of $F$ at $\lambda = 1$. Furthermore, $\gamma$ has finite arc length if $DF(\bar{x})$ is nonsingular.

Lemma 3 is a special case of the following more general lemma.

*Lemma 4.* Let $F : E^p \to E^p$ be a $C^2$ map such that for some $r > 0$ and $\tilde{r} > 0$, $F(x)$ and $x - a$ do not point in opposite directions for $\|x\| = r$, $\|a\| < \tilde{r}$. Then $F$ has a zero in $\{x \in E^p \mid \|x\| \leq r\}$, and for almost all $a \in E^p$, $\|a\| < \tilde{r}$, there is a zero curve $\gamma$ of

$$\rho_a(\lambda, x) = \lambda F(x) + (1-\lambda)(x-a),$$

along which the Jacobian matrix $D\rho_a(\lambda, x)$ has full rank, emanating from $(0,a)$ and reaching a zero $\bar{x}$ of $F$ at $\lambda = 1$. Furthermore, $\gamma$ has finite arc length if $DF(\bar{x})$ is nonsingular.

*Theorem 1.* Let $N(Y)$ in (7) be a $C^2$ mapping, and suppose there exist constants $C$ and $\nu$ such that

$$\limsup_{\|Y\|_\infty \to \infty} \frac{\|N(Y)\|_\infty}{\|Y\|_\infty^\nu} = C, \qquad 0 \leq \nu < 1. \tag{8}$$

For $W \in E^p$, define $\rho_W : [0,1) \times E^p \to E^p$ by

$$\rho_W(\lambda, Y) = \lambda\, F(Y) + (1-\lambda)(Y - W).$$

Then for almost all $W \in E^p$ there exists a zero curve $\gamma$ of $\rho_W$, along which the Jacobian matrix $D\rho_W(\lambda, Y)$ has full rank, emanating from $(0, W)$ and reaching a zero $\tilde{Y}$ of $F$ (at $\lambda = 1$). Furthermore, if $DF(\tilde{Y})$ is nonsingular, then $\gamma$ has finite arc length.

*Proof.* As observed above, the matrix $M$ in (7) is a P-matrix. One of the useful properties of P-matrices is the sign-reversal property [10]: for any $Y \neq 0$ there is an index $j$ such that $Y_j (MY)_j > 0$. A simple compactness argument shows that

$$\min_{\|Y\|_\infty = 1} \max_{1 \leq j \leq p} Y_j (MY)_j = \Gamma > 0. \tag{9}$$

Choose $\epsilon > 0$. Using (9) and $Y = \|Y\|_\infty (Y / \|Y\|_\infty)$ yields

$$\max_j (Y - W)_j (MY + N(Y))_j \geq \Gamma \|Y\|_\infty^2 - \|Y\|_\infty (C + \epsilon) \|Y\|_\infty^\nu$$
$$- \|W\|_\infty \|M\|_\infty \|Y\|_\infty - \|W\|_\infty (C + \epsilon) \|Y\|_\infty^\nu > 0$$

for $\|W\|_\infty$ bounded and $\|Y\|_\infty$ sufficiently large. Therefore for any $\tilde{r} > 0$ there exists $r > 0$ such that $Y - W$ and $F(Y) = MY + N(Y)$ do not point in opposite directions for $\|Y\|_\infty = r$ and $\|W\|_\infty < \tilde{r}$. The result now follows directly from Lemma 4. *Q.E.D*

*Corollary 1.* Let $N(Y)$ in (7) be a $C^2$ mapping and $\Gamma > 0$ defined by (9). If

$$\limsup_{\|Y\|_\infty \to \infty} \frac{\|N(Y)\|_\infty}{\|Y\|_\infty} = C < \Gamma,$$

then the conclusion of Theorem 1 holds.

*Corollary 2.* If $f(x, y, y')$ in (1) is $C^2$ and bounded, then the conclusion of Theorem 1 holds.

*Corollary 3.* Let $f(x, y, y')$ in (1) be a $C^2$ mapping, and suppose there exist constants $\mu$ and $\nu$ such that

$$\limsup_{\|y\|_\infty \to \infty} \max_{\substack{0 \leq x \leq 1 \\ u \in E^n}} \frac{\|f(x, y, u)\|_\infty}{\|y\|_\infty^\nu} = \mu, \quad 0 \leq \nu < 1.$$

Then the conclusion of Theorem 1 holds.

*Proof.* Let

$$y_k = \sum_{i=1}^{n+2} Y_{(k-1)(n+2)+i} B_i(x), \quad k = 1, \ldots, \hat{n}, \quad 0 \leq x \leq 1.$$

Because the B-splines $B_i(x)$ are a partition of unity [8], $|y_k| \leq \|Y\|_\infty$ for each $k$ and thus $\|y\|_\infty \leq \|Y\|_\infty$. The B-splines are also well-conditioned in the sense that there exists a constant $D$ such that [8]

$$\|Y\|_\infty \leq D \|y\|_\infty .$$

Thus, given $\epsilon > 0$,

$$\frac{\|f(x, y, u)\|_\infty}{\|Y\|_\infty^\nu} \leq \mu + \epsilon$$

for $\|Y\|_\infty$ sufficiently large (note that $\|Y\|_\infty$ large implies $\|y\|_\infty$ large). Now from the definitions of $y$ and $N(Y)$, it follows that

$$\frac{\|N(Y)\|_\infty}{\|Y\|_\infty^\nu} \leq \mu + \epsilon$$

for $\|Y\|_\infty$ large enough, which is precisely the condition (8) in Theorem 1 (for some constant $C \leq \mu$). *Q.E.D.*

**3. Algorithm.** The general idea of the algorithm is apparent from Theorem 1: just follow the zero curve $\gamma$ emanating from $(0, W)$ until a zero $\tilde{Y}$ of $F(Y)$ is reached (at $\lambda = 1$). Of course it is nontrivial to develop a viable numerical algorithm based on that idea, but at least conceptually, the algorithm for solving the nonlinear system of equations (7) is clear and simple. The homotopy map is

$$\rho_W(\lambda, Y) = \lambda F(Y) + (1 - \lambda)(Y - W), \tag{10}$$

which has the same form as a standard continuation or embedding mapping. However, there are two crucial differences. In standard continuation, the embedding parameter $\lambda$ increases monotonically from 0 to 1 as the trivial problem $Y - W = 0$ is continuously deformed to the problem $F(Y) = 0$. The present homotopy method permits $\lambda$ to both increase and decrease along $\gamma$ with no adverse effect; that is, turning points present no special difficulty. The second important difference is that there are never any "singular points" which afflict standard continuation methods. The way in which the zero curve $\gamma$ of $\rho_W$ is followed and the full rank of $D\rho_W$ along $\gamma$ guarantee this. Observe that Lemma 1 guarantees that $\gamma$ cannot just "stop" at an interior point of $[0, 1) \times E^p$.

The zero curve $\gamma$ of the homotopy map $\rho_W(\lambda, Y)$ in (10) can be tracked by many different techniques; refer to the excellent survey [1] and recent work by Rheinboldt and Burkhardt[22] and Mejia[16]. The numerical results presented later were obtained with the software package HOMPACK, currently under development at Sandia National Laboratories, General Motors Research Laboratories, and Virginia Polytechnic Institute and State University. HOMPACK is a suite of codes for tracking zero curves of probability one homotopy maps, and provides both high level and low level subroutines for three different approaches to tracking $\gamma$. The three algorithmic approaches provided by HOMPACK are: 1) an ODE-based algorithm based on that in [34], with several refinements; 2) a predictor-corrector algorithm whose corrector follows the flow normal to the Davidenko flow (a "normal flow" algorithm); 3) a version of Rheinboldt's linear predictor, quasi-Newton corrector algorithm [22] (an "augmented Jacobian" method). HOMPACK also provides qualitatively different algorithms for dense and sparse Jacobian matrices, but sparsity will not be discussed here.

First the ODE-based algorithm will be discussed. Assuming that $F(Y)$ is $C^2$ and $W$ is such that Theorem 1 holds, the zero curve $\gamma$ is $C^1$ and can be parametrized by arc length $s$. Thus $\lambda = \lambda(s)$, $Y = Y(s)$ along $\gamma$, and

$$\rho_W(\lambda(s), Y(s)) = 0 \tag{11}$$

identically in $s$. Therefore

$$\frac{d}{ds}\rho_W(\lambda(s), Y(s)) = D\rho_W(\lambda(s), Y(s)) \begin{pmatrix} \frac{d\lambda}{ds} \\ \frac{dY}{ds} \end{pmatrix} = 0, \tag{12}$$

$$\left\| \left( \frac{d\lambda}{ds}, \frac{dY}{ds} \right) \right\|_2 = 1. \tag{13}$$

If we take

$$\lambda(0) = 0, \quad Y(0) = W, \tag{14}$$

the zero curve $\gamma$ is the trajectory of the initial value problem (12–14). When $\lambda(\bar{s}) = 1$, the corresponding $Y(\bar{s})$ is a zero of $F(Y)$. Thus all the sophisticated ODE techniques currently available can be brought to bear on the problem of tracking $\gamma$ [26], [35].

ODE software requires $(d\lambda/ds, dY/ds)$ explicitly, and (12), (13) only implicitly define the derivative $(d\lambda/ds, dY/ds)$. This can be calculated by finding the kernel of the $p \times (p+1)$ Jacobian matrix

$$D\rho_W(\lambda(s), Y(s)),$$

which has full rank by Theorem 1. It is here that a substantial amount of computation is incurred, and it is imperative that the number of derivative evaluations be kept small. Once the kernel has been calculated, the derivative $(d\lambda/ds, dY/ds)$ is uniquely determined by (13) and continuity. Complete details for solving the initial value problem (12–14) and obtaining $Y(\bar{s})$ are in [34] and [35].

Remember that tracking $\gamma$ was merely a means to an end, namely a zero $\bar{Y}$ of $F(Y)$. Since $\gamma$ itself is of no interest (usually), one should not waste computational effort following it too closely. However, since $\gamma$ is the only sure way to $\bar{Y}$, losing $\gamma$ can be disastrous. The tradeoff between computational efficiency and reliability is very delicate, and a fool-proof strategy appears difficult to achieve. This is the reason HOMPACK provides several algorithms; no single algorithm is superior overall, and each of the three beats the other two (sometimes by an order of magnitude) on particular problems.

The normal flow algorithm has three phases: prediction, correction, and step size estimation. (10) and (11) are the relevant equations here. For the prediction phase, assume that several points $P^{(1)} = (\lambda(s_1), Y(s_1))$, $P^{(2)} = (\lambda(s_2), Y(s_2))$ on $\gamma$ with corresponding tangent vectors $(d\lambda/ds(s_1), dY/ds(s_1))$, $(d\lambda/ds(s_2), dY/ds(s_2))$ have been found, and $h$ is an estimate of the optimal step (in arc length) to take along $\gamma$ . The prediction of the next point on $\gamma$ is

$$Z^{(0)} = p(s_2 + h), \tag{15}$$

where $p(s)$ is the Hermite cubic interpolating $(\lambda(s), Y(s))$ at $s_1$ and $s_2$. Precisely,

$$\begin{aligned} p(s_1) &= (\lambda(s_1), Y(s_1)), \quad p'(s_1) = (d\lambda/ds(s_1), dY/ds(s_1)), \\ p(s_2) &= (\lambda(s_2), Y(s_2)), \quad p'(s_2) = (d\lambda/ds(s_2), dY/ds(s_2)), \end{aligned}$$

and each component of $p(s)$ is a polynomial in $s$ of degree less than or equal to 3.

Starting at the predicted point $Z^{(0)}$, the corrector iteration is

$$Z^{(n+1)} = Z^{(n)} - \left[ D\rho_W\left(Z^{(n)}\right) \right]^{\dagger} \rho_W\left(Z^{(n)}\right), \qquad n = 0, 1, \ldots \tag{16}$$

where $[D\rho_W(Z^{(n)})]^\dagger$ is the Moore-Penrose pseudoinverse of the $p \times (p+1)$ Jacobian matrix $D\rho_W$. Small perturbations of $W$ produce small changes in the trajectory $\gamma$, and the family of trajectories $\gamma$ for varying $W$ is known as the "Davidenko flow". Geometrically, the iterates given by (16) return to the zero curve along the flow normal to the Davidenko flow, hence the name "normal flow algorithm".

A corrector step $\Delta Z$ is the unique minimum norm solution of the equation

$$[D\rho_W]\Delta Z = -\rho_W. \tag{17}$$

Fortunately $\Delta Z$ can be calculated at the same time as the kernel of $[D\rho_W]$, and with just a little more work. Normally for dense problems the kernel of $[D\rho_W]$ is found by computing a QR factorization of $[D\rho_W]$, and then using back substitution. By applying this QR factorization to $-\rho_W$ and using back substitution again, a *particular* solution $v$ to (17) can be found. Let $u \neq 0$ be any vector in the kernel of $[D\rho_W]$. Then the minimum norm solution of (17) is

$$\Delta Z = v - \frac{v^t u}{u^t u} u. \tag{18}$$

Since the kernel of $[D\rho_W]$ is needed anyway for the tangent vectors, solving (17) only requires another $O(p^2)$ operations beyond those for the kernel. The number of iterations required for convergence of (16) should be kept small (say $< 4$) since QR factorizations of $[D\rho_W]$ are expensive. The alternative of using $[D\rho_W(Z^{(0)})]$ for several iterations, which results in linear convergence, is rarely cost effective.

When the iteration (16) converges, the final iterate $Z^{(n+1)}$ is accepted as the next point on $\gamma$, and the tangent vector to the integral curve through $Z^{(n)}$ is used for the tangent–this saves a Jacobian matrix evaluation and factorization at $Z^{(n+1)}$. The step size estimation described next attempts to balance progress along $\gamma$ with the effort expended on the iteration (16).

Define a contraction factor

$$L = \frac{\|Z^{(2)} - Z^{(1)}\|}{\|Z^{(1)} - Z^{(0)}\|}, \tag{19}$$

a residual factor

$$R = \frac{\|\rho_W(Z^{(1)})\|}{\|\rho_W(Z^{(0)})\|}, \tag{20}$$

a distance factor ($Z^* = \lim_{n\to\infty} Z^{(n)}$)

$$D = \frac{\|Z^{(1)} - Z^*\|}{\|Z^{(0)} - Z^*\|}, \tag{21}$$

and ideal values $\bar{L}$, $\bar{R}$, $\bar{D}$ for these three. Let $h$ be the current step size (the distance from $Z^*$ to the previous point found on $\gamma$), and $\bar{h}$ the "optimal" step size for the next step. The goal is to achieve

$$\frac{\bar{L}}{L} \approx \frac{\bar{R}}{R} \approx \frac{\bar{D}}{D} \approx \frac{\bar{h}^q}{h^q} \tag{22}$$

for some $q$. This leads to the choice

$$\hat{h} = \left(\min\{\bar{L}/L, \bar{R}/R, \bar{D}/D\}\right)^{1/q} h, \tag{23}$$

a worst case choice. To prevent chattering and unreasonable values, constants $h_{\min}$ (minimum allowed step size), $h_{\max}$ (maximum allowed step size), $B_{\min}$ (contraction factor), and $B_{\max}$ (expansion factor) are chosen, and $\bar{h}$ is taken as

$$\bar{h} = \min\left\{\max\{h_{\min}, B_{\min}h, \hat{h}\}, B_{\max}h, h_{\max}\right\}. \tag{24}$$

There are eight parameters in this process: $\bar{L}$, $\bar{R}$, $\bar{D}$, $h_{\min}$, $h_{\max}$, $B_{\min}$, $B_{\max}$, $q$. HOMPACK permits the user to specify nondefault values for any of these. The choice of $\bar{h}$ from (24) can be refined further. If (16) converged in one iteration, then $\bar{h}$ should certainly not be smaller than $h$, hence set

$$\bar{h} := \max\{h, \bar{h}\} \tag{25}$$

if (16) only required one iteration.

To prevent divergence from the iteration (16), if (16) has not converged after $K$ iterations, $h$ is halved and a new prediction is computed. Every time $h$ is halved the old value $h_{\text{old}}$ is saved. Thus if (16) has failed to converge in $K$ iterations sometime during this step, the new $\bar{h}$ should not be greater than the value $h_{\text{old}}$ known to produce failure. Hence in this case

$$\bar{h} := \min\{h_{\text{old}}, \bar{h}\}. \tag{26}$$

Finally, if (16) required the maximum $K$ iterations, the step size should not increase, so in this case set

$$\bar{h} := \min\{h, \bar{h}\}. \tag{27}$$

The logic in (25–27) is rarely invoked, but it does have a stabilizing effect on the algorithm.

Rheinboldt's augmented Jacobian algorithm together with step size strategies has been described very well elsewhere [22], and will not be repeated here.

**4. Numerical results.** Consider the nonlinear two-point boundary value problem [24]

$$\psi''' = \frac{\eta - 3}{2}\psi\psi'' - \eta(\psi')^2 + 1 - G^2 + s\psi' \tag{28}$$

$$G'' = \frac{\eta - 3}{2}\psi G' - (\eta - 1)\psi' G + s(G - 1) \tag{29}$$

$$\psi(0) = \psi'(0) = G(0) = 0 \tag{30}$$

$$\psi'(\infty) = 0, \quad G(\infty) = 1 \tag{31}$$

where $\eta$ and $s$ are fixed constants. For the purposes of comparison and discussion, this difficult problem will be solved (or attempted) by several different methods. All the computations were done

with FORTRAN 77 (using the optimizing compilers) on a VAX 11/780 and an Elxsi 6400, and CPU times are reported in seconds.

## SIMPLE SHOOTING

Let $\psi(r;v)$, $G(r;v)$ be the solution to the initial value problem (28–29) with initial conditions (30) and

$$v = \begin{pmatrix} \psi''(0) \\ G'(0) \end{pmatrix}. \tag{32}$$

Then the original two-point boundary value problem (28–31) is equivalent to the nonlinear system of equations

$$\hat{F}(v) = \begin{pmatrix} \psi'(L;v) \\ G(L;v) - 1 \end{pmatrix} = 0 \tag{33}$$

for $L = \infty$ (in practice $L$ is taken to be some sufficiently large finite number). The standard homotopy map for solving equation (33) is

$$\lambda \hat{F}(v) + (1-\lambda)(v-a). \tag{34}$$

The difficulty with the homotopy map (34) is that for most values of $v$ the vector $\hat{F}(v)$ is huge, and computations with (34) frequently produce overflow. For example, with $\eta = 3.0$, $s = 0$, $a = 0$, and $L = 6.25$ (not large enough), a solution to (33) can be obtained. However, for $L = 6.5$ (still not large enough), the calculation of $\hat{F}(v)$ in (34) produces overflow on the VAX 11/780.

Another natural homotopy map to try is

$$\begin{pmatrix} \psi'(\lambda L;v) \\ G(\lambda L;v) - \lambda \end{pmatrix} + (1-\lambda)(v-a), \tag{35}$$

which enforces the boundary condition $G(L;v) = 1$ gradually and also increases the interval length gradually. For $\eta = 3.0$, $s = 0$, $a = 0$, and $L = 9.0$, the homotopy map (35) also causes overflow on the VAX 11/780.

## MULTIPLE SHOOTING

Simple shooting with bad estimates of the initial conditions is obviously susceptible to numerical difficulties, and the idea of multiple shooting is to decrease the size of the integration intervals, thereby keeping the shooting trajectories bounded. The tradeoff is that the dimension of the nonlinear problem to be solved increases.

Divide the interval $[0, L]$ into $m$ equal subintervals, and let

$$r_k = kL/m, \qquad k = 1, \ldots, m.$$

The vector of unknowns in (32) is generalized to

$$
\begin{aligned}
(36) \qquad v = \big(&\psi''(0), G'(0), \psi(\tau_1), \psi'(\tau_1), \psi''(\tau_1), G(\tau_1), G'(\tau_1), \\
&\psi(\tau_2), \psi'(\tau_2), \psi''(\tau_2), G(\tau_2), G'(\tau_2), \\
&\vdots \\
&\psi(\tau_{m-1}), \psi'(\tau_{m-1}), \psi''(\tau_{m-1}), G(\tau_{m-1}), G'(\tau_{m-1})\big),
\end{aligned}
$$

which has dimension $5m - 3$. The concept of multiple shooting is to shoot over each subinterval separately, and then match the solutions at the boundary points $\tau_1, \ldots, \tau_{m-1}$, as well as matching the boundary conditions at $\tau_m = L$. Let

$$
(37) \qquad v_{[k,l]} = (v_k, v_{k+1}, \ldots, v_l)
$$

be a vector formed from the components of $v$. Let

$$
(38) \qquad \psi\big(\tau; v_{[k,l]}, \varsigma\big), \qquad G\big(\tau; v_{[k,l]}, \varsigma\big)
$$

be the solution of equations (28–29) with initial conditions $v_{[k,l]}$ at $\tau = \varsigma$ (for $k = 1$, $l = 2$, the initial conditions (30) are also used). Then the original two-point boundary value problem (28–31) is equivalent to the nonlinear system of equations

$$
\begin{aligned}
(39)\ \hat{F}(v) = \big(&\psi(\tau_1; v_{[1,2]}, 0) - v_3,\ \psi'(\tau_1; v_{[1,2]}, 0) - v_4,\ \psi''(\tau_1; v_{[1,2]}, 0) - v_5, \\
&G(\tau_1; v_{[1,2]}, 0) - v_6,\ G'(\tau_1; v_{[1,2]}, 0) - v_7, \\
&\psi(\tau_2; v_{[3,7]}, \tau_1) - v_8,\ \psi'(\tau_2; v_{[3,7]}, \tau_1) - v_9,\ \psi''(\tau_2; v_{[3,7]}, \tau_1) - v_{10}, \\
&G(\tau_2; v_{[3,7]}, \tau_1) - v_{11},\ G'(\tau_2; v_{[3,7]}, \tau_1) - v_{12}, \\
&\vdots \\
&\psi(\tau_{m-1}; v_{[5m-12,5m-8]}, \tau_{m-2}) - v_{5m-7},\ \psi'(\tau_{m-1}; v_{[5m-12,5m-8]}, \tau_{m-2}) - v_{5m-6}, \\
&\psi''(\tau_{m-1}; v_{[5m-12,5m-8]}, \tau_{m-2}) - v_{5m-5},\ G(\tau_{m-1}; v_{[5m-12,5m-8]}, \tau_{m-2}) - v_{5m-4}, \\
&G'(\tau_{m-1}; v_{[5m-12,5m-8]}, \tau_{m-2}) - v_{5m-3},\ \psi'(\tau_m; v_{[5m-7,5m-3]}, \tau_{m-1}), \\
&G(\tau_m; v_{[5m-7,5m-3]}, \tau_{m-1}) - 1\big) = 0.
\end{aligned}
$$

The homotopy map used for solving equation (39) is

$$
(40) \qquad \lambda \hat{F}(v) + (1 - \lambda)(v - a).
$$

Multiple shooting can be made to work for the problem (28–31), but it turns out that the starting point must be rather close to the solution. The solutions $\psi(\tau)$, $G(\tau)$ grow rapidly on the subintervals, and even though the subintervals are small, poor estimates of the initial conditions in just a few subintervals result in machine floating-point overflow and failure of the whole scheme. The shortcoming is not in the homotopy map (40) but in simply evaluating $\hat{F}(v)$ in (39). For example, with $\eta = -.1$, $s = 2.0$, $L = 12$, $v = 0$ (a very easy case for the spline collocation method discussed next, according to Figure 3), multiple shooting failed to reach the solution in 4 hours of CPU time

on a VAX 11/780 for both $m = 6$ and $m = 12$, and produced overflow for $m = 4$. Spline collocation for the same data (using $n = 50$) converged easily and required 43.5 min.

## CUBIC SPLINE COLLOCATION

For the interval $[0, L]$ take the mesh points

$$x_0 = 0, x_1 = \delta, x_k = x_{k-1} + h, \quad k = 2, \ldots, n, \qquad x_{n+1} = x_n + \delta = L$$

with $0 < \delta \ll h$. Let $B_i(x)$ denote the $i$th B-spline of order 4 defined on the knot sequence $x_0$, $x_0$, $x_0$, $x_0$, $x_2$, $x_3$, ..., $x_{n-2}$, $x_{n-1}$, $\tilde{x}_{n+1}$, $\tilde{x}_{n+1}$, $\tilde{x}_{n+1}$, $\tilde{x}_{n+1}$, where $\tilde{x}_{n+1} = x_{n+1} + \delta$, $\delta \ll h$. This B-spline basis $\{B_i\}$ has dimension $n + 2$. Substituting the approximations

$$\psi(x) \approx A(x) = \sum_{i=1}^{n+2} \alpha_i B_i(x) \tag{41}$$

$$\psi'(x) \approx B(x) = \sum_{i=1}^{n+2} \beta_i B_i(x) \tag{42}$$

$$G(x) \approx C(x) = \sum_{i=1}^{n+2} \gamma_i B_i(x) \tag{43}$$

into equations (28–31) yields the nonlinear system of equations

$$\begin{aligned}
A(x_0) &= 0 \\
A''(x_j) &= B'(x_j), \quad j = 1, \ldots, n \\
A'(x_{n+1}) &= B(x_{n+1}) \\
B(x_0) &= 0 \\
B''(x_j) &= \frac{\eta - 3}{2} A(x_j) B'(x_j) - \eta B(x_j)^2 + 1 - C(x_j)^2 + \varepsilon B(x_j), \quad j = 1, \ldots, n \\
B(x_{n+1}) &= 0 \\
C(x_0) &= 0 \\
C''(x_j) &= \frac{\eta - 3}{2} A(x_j) C'(x_j) - (\eta - 1) B(x_j) C(x_j) + \varepsilon (C(x_j) - 1), \quad j = 1, \ldots, n \\
C(x_{n+1}) &= 1.
\end{aligned} \tag{44}$$

Let $Y = (\alpha_1, \ldots, \alpha_{n+2}, \beta_1, \ldots, \beta_{n+2}, \gamma_1, \ldots, \gamma_{n+2})^t$. Then the system (44) has the form

$$F(Y) = MY + N(Y) = 0, \tag{45}$$

where

$$M = \begin{pmatrix} M^{(1)} & 0 & 0 \\ 0 & M^{(2)} & 0 \\ 0 & 0 & M^{(3)} \end{pmatrix},$$

$$M^{(1)} = \begin{bmatrix} \sigma_1 B_1(x_0) & 0 & 0 & 0 & 0 & \cdots \\ -B_1''(x_1) & -B_2''(x_1) & -B_3''(x_1) & -B_4''(x_1) & 0 & \cdots \\ 0 & -B_2''(x_2) & -B_3''(x_2) & -B_4''(x_2) & 0 & \cdots \\ 0 & 0 & -B_3''(x_3) & -B_4''(x_3) & -B_5''(x_3) & \cdots \\ & & & & & \ddots \\ \cdots & 0 & -B_{n-1}''(x_{n-1}) & -B_n''(x_{n-1}) & -B_{n+1}''(x_{n-1}) & 0 \\ \cdots & 0 & -B_{n-1}''(x_n) & -B_n''(x_n) & -B_{n+1}''(x_n) & -B_{n+2}''(x_n) \\ \cdots & 0 & \sigma_2 B_{n-1}'(x_{n+1}) & \sigma_2 B_n'(x_{n+1}) & \sigma_2 B_{n+1}'(x_{n+1}) & \sigma_2 B_{n+2}'(x_{n+1}) \end{bmatrix}$$

$$M^{(2)} = M^{(3)}$$

$$= \begin{bmatrix} \sigma_1 B_1(x_0) & 0 & 0 & 0 & 0 & \cdots \\ -B_1''(x_1) & -B_2''(x_1) & -B_3''(x_1) & -B_4''(x_1) & 0 & \cdots \\ 0 & -B_2''(x_2) & -B_3''(x_2) & -B_4''(x_2) & 0 & \cdots \\ 0 & 0 & -B_3''(x_3) & -B_4''(x_3) & -B_5''(x_3) & \cdots \\ & & & & & \ddots \\ \cdots & 0 & -B_{n-1}''(x_{n-1}) & -B_n''(x_{n-1}) & -B_{n+1}''(x_{n-1}) & 0 \\ \cdots & 0 & -B_{n-1}''(x_n) & -B_n''(x_n) & -B_{n+1}''(x_n) & -B_{n+2}''(x_n) \\ \cdots & 0 & \sigma_3 B_{n-1}(x_{n+1}) & \sigma_3 B_n(x_{n+1}) & \sigma_3 B_{n+1}(x_{n+1}) & \sigma_3 B_{n+2}(x_{n+1}) \end{bmatrix}$$

$$\sigma_1,\ \sigma_2,\ \sigma_3 > 0,$$

$$\begin{aligned} N(Y) = \big(&0, B'(x_1), B'(x_2), \ldots, B'(x_n), -\sigma_2 B(x_{n+1}), \\ &0, \frac{\eta-3}{2} A(x_1)B'(x_1) - \eta B(x_1)^2 + 1 - C(x_1)^2 + s B(x_1), \ldots, \\ &\frac{\eta-3}{2} A(x_n)B'(x_n) - \eta B(x_n)^2 + 1 - C(x_n)^2 + s B(x_n), 0, \\ &0, \frac{\eta-3}{2} A(x_1)C'(x_1) - (\eta-1)B(x_1)C(x_1) + s(C(x_1)-1), \ldots, \\ &\frac{\eta-3}{2} A(x_n)C'(x_n) - (\eta-1)B(x_n)C(x_n) + s(C(x_n)-1), -\sigma_3\big). \end{aligned}$$

Because of the B-spline property

$$\sum_{i=1}^{n+2} B_i(x) = 1, \qquad x_0 < x < \tilde{x}_{n+1},$$

and the concavity of cubic B-splines at the center of their support, the matrices $M^{(1)}$, $M^{(2)}$, and $M^{(3)}$ are row diagonally dominant with positive diagonal elements (for $\delta$ small). By scaling the first and last rows of the $M^{(j)}$ by the $\sigma_k$, each $M^{(j)}$ can be made positive definite. (Note that the more obvious spacing $x_k = k\,h$, $k = 0, 1, \ldots, n+1$, produces a matrix $M^{(1)}$ which is *not* row diagonally dominant and *not* positive definite after row scaling.) Because of the B-splines' local support, $M$ is a banded matrix. However, because of the nonlinear coupling between $A$, $B$, and $C$ in (44), the Jacobian matrix of $N(Y)$ has the form

$$DN(Y) = \begin{pmatrix} \mathcal{B} & \mathcal{B} & \mathcal{B} \\ \mathcal{B} & \mathcal{B} & \mathcal{B} \\ \mathcal{B} & \mathcal{B} & \mathcal{B} \end{pmatrix},$$

where the $B$'s are (different) banded matrices. The diagonal $B$ blocks, as well as the entire matrix $DN(Y)$, may be indefinite or singular. Furthermore, the matrix $M + DN(Y)$ may be indefinite or singular. These facts make it difficult to exploit the sparsity of $DN(Y)$, and suggest that a higher order spline approximation resulting in a smaller, denser matrix $DN(Y)$ may be preferable.

Consider then the same mesh points $x_0, \ldots, x_{n+1}$ mentioned earlier, and let $B_i$ be the $i$th B-spline of order 6 (a quintic) defined on the knot sequence

$$x_0, x_0, x_0, x_0, x_0, x_0, x_3, x_4, \ldots, x_{n-3}, x_{n-2}, \tilde{x}_{n+1}, \tilde{x}_{n+1}, \tilde{x}_{n+1}, \tilde{x}_{n+1}, \tilde{x}_{n+1}, \tilde{x}_{n+1}.$$

As before, this B-spline vector space has dimension $n+2$. Using the approximations (41–43) results in the same nonlinear system of equations (44) for the spline coefficients as before, although of course $A$, $B$, and $C$ are now quintic splines instead of cubic splines. The matrix $M$ in (45) is now row diagonally dominant with positive diagonal elements, but cannot necessarily be made positive definite by scaling the rows corresponding to the boundary conditions. However, $M$ is a P-matrix (all principal minors are positive), and such matrices behave essentially like positive definite matrices as far as homotopy methods are concerned [36].

For the problem (28-31) $L$ must be large (from 10 to 200) and most of the action in the solution $\psi(x)$, $G(x)$ occurs for small $x$. Hence an unequally spaced mesh is appropriate, and the following mesh was used (this uneven mesh does not qualitatively change $M$):

$$x_0 = 0, x_k = e^{(k-1)\Delta x} - 1 + \delta, \quad k = 1, \ldots, n, \quad x_{n+1} = x_n + \delta,$$

where $\Delta x = \ln(L + 1 - 2\delta)/(n-1)$ and $\delta = 10^{-6}$.

Figure 1 shows the solution $A(x) \approx \psi(x)$ for different values of the interval length $L$. The solution $A(x) \approx \psi(x)$ appears to level off around $L = 11$, and this value for $L$ has been reported in the literature [24]. However, the solution for $L = 14$ suggests that this $L$ is not large enough, or else there is nonuniqueness of solutions. Figure 2 shows the effect of $n$ on the solution $A(x) \approx \psi(x)$, which clearly is converging as $n$ increases. Figure 3 shows the effect of the parameter $s$ on the solution $A(x) \approx \psi(x)$. Note that the problem becomes more difficult as $s \to 0$, and the solution is very sensitive to $s$ for $s < 1$. Figure 5 is the analog of Figure 3 for $G(x)$. It is evident that $L \gg 12$ is going to be necessary for $s < 1$.

Figure 4 shows the dependence of the solution $A(x) \approx \psi(x)$ on the parameter $\eta$. The problem becomes more difficult as $\eta$ increases from $-1$ toward 0, and is extremely difficult for $\eta$ near 0 with a small $s = .05$. Note the sensitivity of the solution $A(x) \approx \psi(x)$ with respect to $\eta$ for $\eta > -1.0$. Figure 6, showing $G(x)$, corresponds to Figure 4. For these cases $L = 20$ appears to be adequate.

Figure 7 shows a problem inherent in most nonlinear discretizations of nonlinear problems–multiple solutions. Both of these solutions were obtained with the homotopy method (from different starting points), and are qualitatively very different. The degenerate case $\eta = s = 0$ is very interesting, but was not pursued any further in this work.

Figure 8 shows the solution $A(x) \approx \psi(x)$ for $\eta = 0.261$ and $s = .05$, an extremely difficult case. The solutions $A(x)$ are extremely sensitive to $\eta$ for $\eta > 0$. For example, with $s = .05$, $n = 70$, $L = 200$, and starting at the solution for the case $\eta = 0.225$, the arc length to the solution

for $\eta = 0.250$ was greater than 37, and the homotopy algorithm required 111 Jacobian matrix evaluations. The solution was obtained with a relative error of $10^{-9}$, and the zero curve was tracked with a local error criterion of $10^{-5}$.

## REFERENCES


[1] E. ALLGOWER AND K. GEORG, *Simplicial and continuation methods for approximating fixed points*, SIAM Rev., 22 (1980), pp. 28–85.

[2] U. ASCHER, *Solving boundary-value problems with a spline-collocation code*, J. Comput. Phys., 34 (1980), p. 401.

[3] U. ASCHER, J. CHRISTIANSEN, AND R. D. RUSSELL, *Collocation software for boundary-value ODEs*, ACM Trans. Math. Software, 7 (1981), pp. 209–222.

[4] U. ASCHER, J. CHRISTIANSEN, AND R. D. RUSSELL, *Algorithm 569. COLSYS: Collocation software for boundary-value ODEs*, ACM Trans. Math. Software, 7 (1981), pp. 223.

[5] P. BOGGS, *The solution of nonlinear systems of equations by A-stable integration techniques*, SIAM J. Numer. Anal., 8 (1971), pp. 767–785.

[6] P. BUSINGER AND G. G. GOLUB, *Linear least squares solutions by Householder transformations*, Numer. Math., 7 (1965), pp. 269–276.

[7] M. E. DAVIS AND G. FAIRWEATHER, *On the use of spline collocation for boundary-value problems arising in chemical engineering*, Comput. Methods Appl. Mech. Engrg., 28 (1981), pp. 179-189.

[8] C. DEBOOR, *A Practical Guide to Splines*, Springer-Verlag, New York, 1978.

[9] B. C. EAVES AND R. SAIGAL, *Homotopies for computation of fixed points on unbounded regions*, Math. Programming, 3 (1972)), pp. 225–237.

[10] M. FIEDLER AND V. PTAK, *On matrices with non-positive off-diagonal elements and positive principal minors*, Czech. Math. J., 12 (1962), pp. 382–400.

[11] K. GEORG, private communication, 1981.

[12] H. B. KELLER, *Numerical Solution of Two-point Boundary Value Problems*, Society for Industrial and Applied Mathematics, Philadelphia, 1976.

[13] ——, *Numerical solution of bifurcation and nonlinear eigenvalue problems*, in Applications of Bifurcation Theory, Academic Press, New York, 1977.

[14] R. W. KLOPFENSTEIN, *Zeros of nonlinear functions*, J. Assoc. Comput. Mech., 8 (1961), pp. 336–373.

[15] M. KUBICEK, *Dependence of solutions of nonlinear systems on a parameter*, ACM-TOMS, 2 (1976), pp. 98–107.

[16] R. MEJIA, *A path following algorithm for partitioned nonlinear systems of equations*, manuscript.

[17] R. MENZEL AND H. SCHWETLICK, *Zur Lösung parameterabhängiger nichtlinearer Gleichungen mit singulären Jacobi-Matrizen*, Numer. Math., 30 (1978), pp. 65–79.

[18] G. MEYER, *On solving nonlinear equations with a one-parameter operator embedding*, SIAM J. Numer. Anal., 5 (1968), pp. 739–752.

[19] J. J. MORÉ, B. S. GARBOW, AND K. E. HILLSTROM, *User Guide for MINPACK-1*, ANL-80-74, Argonne National Laboratory, Argonne, IL (1980).

[20] A. P. MORGAN, *A transformation to avoid solutions at infinity for polynomial systems*, Appl. Math. Comput., to appear.

[21] ——, *A homotopy for solving polynomial systems*, Appl. Math. Comput., to appear.

[22] W. C. RHEINBOLDT AND J. V. BURKARDT, *Algorithm 596: A program for a locally parameterized continuation process*, ACM Trans. Math. Software, 9 (1983), pp. 236-241.

[23] R. SAIGAL AND M. J. TODD, *Efficient acceleration techniques for fixed point algorithms*, SIAM J. Numer. Anal., 15 (1978), pp. 997–1007.

[24] M. R. SCOTT AND H. A. WATTS, *A systematized collection of codes for solving two-point boundary-value problems*, Numerical Methods for Differential Systems, L. Lapidus and W. E. Schiesser, eds., Academic Press, New York, 1976.

[25] ——, *SUPORT—a computer code for two-point boundary value problems via orthonormalization*, SIAM J. Numer. Anal., 14 (1977), pp. 40–70.

[26] L. F. SHAMPINE AND M. K. GORDON, *Computer Solution of Ordinary Differential Equations: The Initial Value Problem*. W. H. Freeman, San Francisco, 1975.

[27] C. Y. WANG AND L. T. WATSON, *Squeezing of a viscous fluid between elliptic plates*, Appl. Sci. Res., 35 (1979), pp. 195–207.

[28] ——, *Viscous flow between rotating discs with injection on the porous disc*, Z. Angew. Math. Phys., 30 (1979), pp. 773–787.

[29] L. T. WATSON, *Numerical study of porous channel flow in a rotating system by a homotopy method*, J. Comput. Appl. Math., 7 (1981), pp. 21–26.

[30] L. T. WATSON, T. Y. LI AND C. Y. WANG, *Fluid dynamics of the ellilptic porous slider*, J. Appl. Mech., 45 (1978), pp. 435–436.

[31] L. T. WATSON AND C. Y. WANG, *Deceleration of a rotating disc in a viscous fluid*, Phys. Fluids, 22 (1979), pp. 2267–2269.

[32] L. T. WATSON AND W. H. YANG, *Optimal design by a homotopy method*, Applicable Anal., 10 (1980), pp. 275–284.

[33] L. T. WATSON, *Computational experience with the Chow-Yorke algorithm*, Math. Programming, 19 (1980), pp. 92–101.

[34] L. T. WATSON AND D. FENNER, *Chow-Yorke algorithm for fixed points of zeros of $C^2$ maps*, ACM TOMS, 6 (1980), pp. 252–260.

[35] L. T. WATSON, *A globally convergent algorithm for computing fixed points of $C^2$ maps*, Appl. Math. Comput., 5 (1979), pp. 297–311.

[36] ——, *Solving the nonlinear complementarity problem by a homotopy method*, SIAM J. Control Optim., 17 (1979), pp. 36–46.

[37] ——, *An algorithm that is globally convergent with probability one for a class of nonlinear two-point boundary value problems*, SIAM J. Numer. Anal., 16 (1979), pp. 394–401.

[38] ——, *Solving finite difference approximations to nonlinear two-point boundary value problems by a homotopy method*, SIAM J. Sci. Stat. Comput., 1 (1980), pp. 467–480.

[39] ——, *Engineering applications of the Chow-Yorke algorithm*, Appl. Math. Comput., 9 (1981), pp. 111–133.

## LIST OF FIGURE CAPTIONS

Figure 1. Solution $A(x) \approx \psi(x)$ for $L = 6$ (solid line), $L = 9$ (dashed), $L = 12$ (short dashed), $L = 14$ (dotted), with $n = 25$, $\eta = -.1$, $s = .2$.

Figure 2. Solution $A(x) \approx \psi(x)$ for $n = 15$ (solid line), $n = 20$ (long dashed), $n = 25$ (short dashed), $n = 50$ (dotted), with $L = 12$, $\eta = -.1$, $s = .2$.

Figure 3. Solution $A(x) \approx \psi(x)$ for $s = .05$ (solid), $s = .2$ (long dashed), $s = 1.0$ (short dashed), $s = 2.0$ (dotted), with $\eta = -.1$, $n = 50$, $L = 12$.

Figure 4. Solution $A(x) \approx \psi(x)$ for $\eta = -2.0$ (solid), $\eta = -1.0$ (long dashed), $\eta = -.1$ (short dashed), with $s = .05$, $n = 50$, $L = 20$.

Figure 5. Solution $C(x) \approx G(x)$ for $s = .05$ (solid), $s = .2$ (long dashed), $s = 1.0$ (short dashed), $s = 2.0$ (dotted), with $\eta = -.1$, $n = 50$, $L = 12$.

Figure 6. Solution $C(x) \approx G(x)$ for $\eta = -2.0$ (solid), $\eta = -1.0$ (long dashed), $\eta = -.1$ (short dashed), with $s = .05$, $n = 50$, $L = 20$.

Figure 7. Two different solutions $A(x) \approx \psi(x)$ for $\eta = s = 0.0$, $n = 15$, $L = 16$.

Figure 8. Solution $A(x) \approx \psi(x)$ for $\eta = 0.261$, $s = .05$, $n = 70$, $L = 200$.

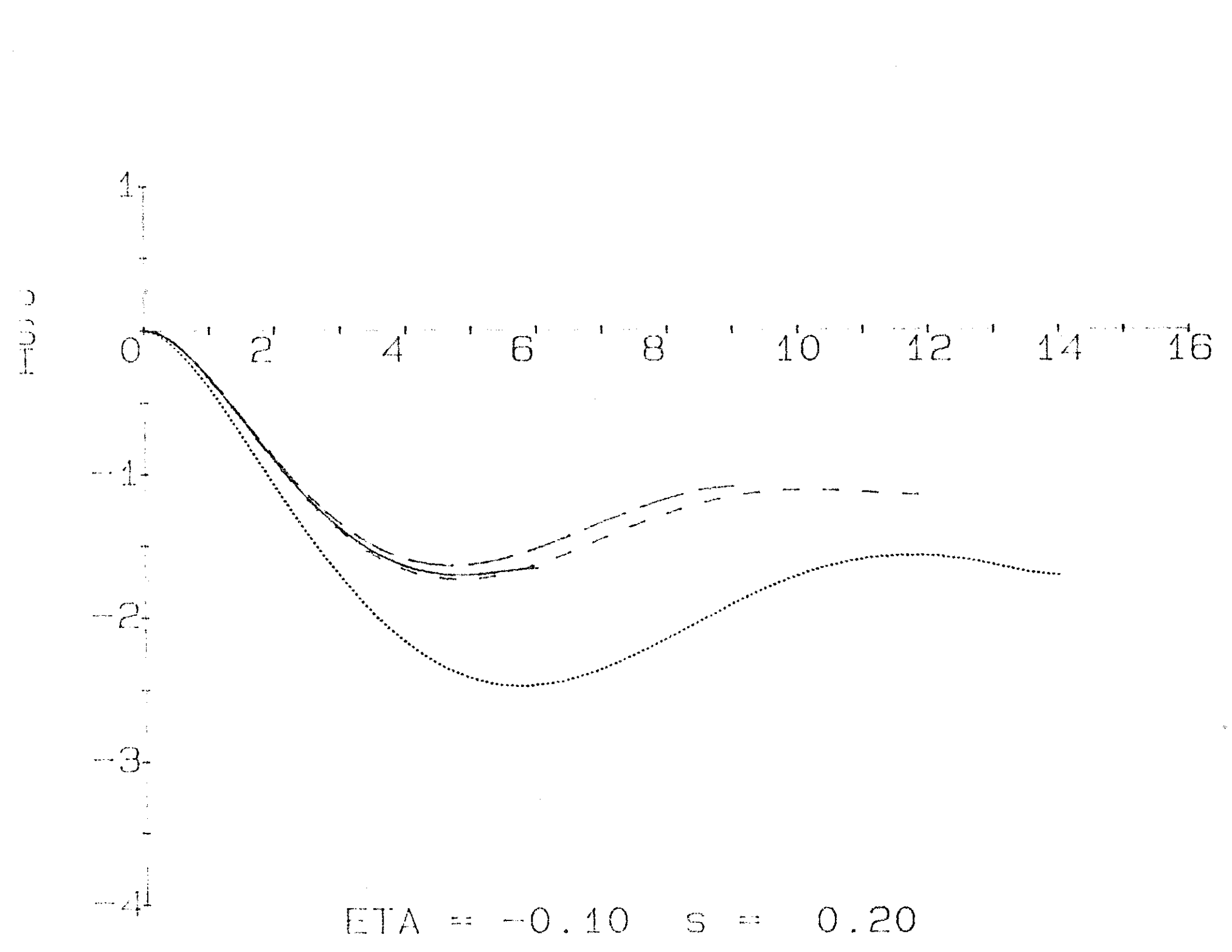


Figure 1

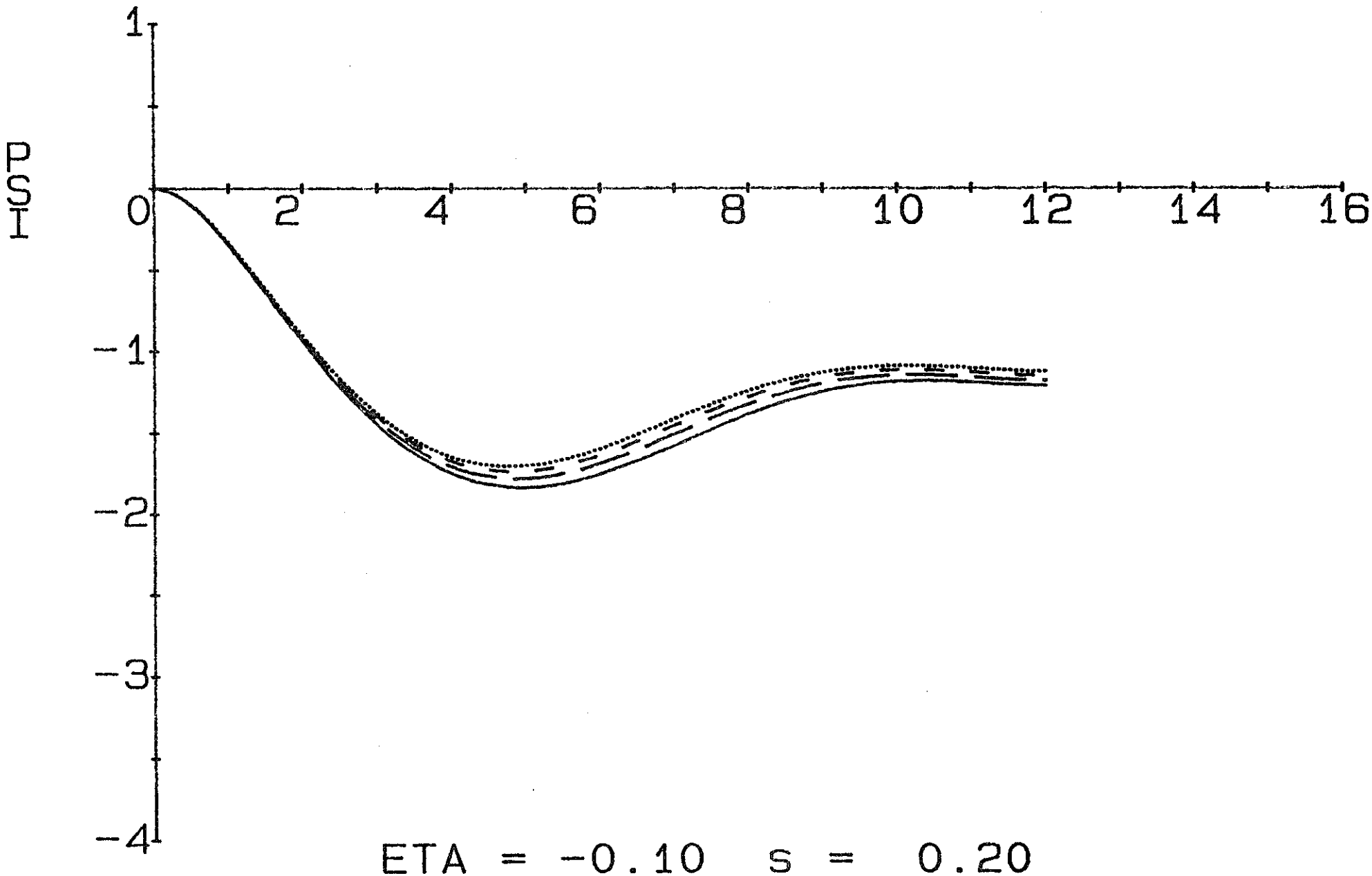


Figure 2

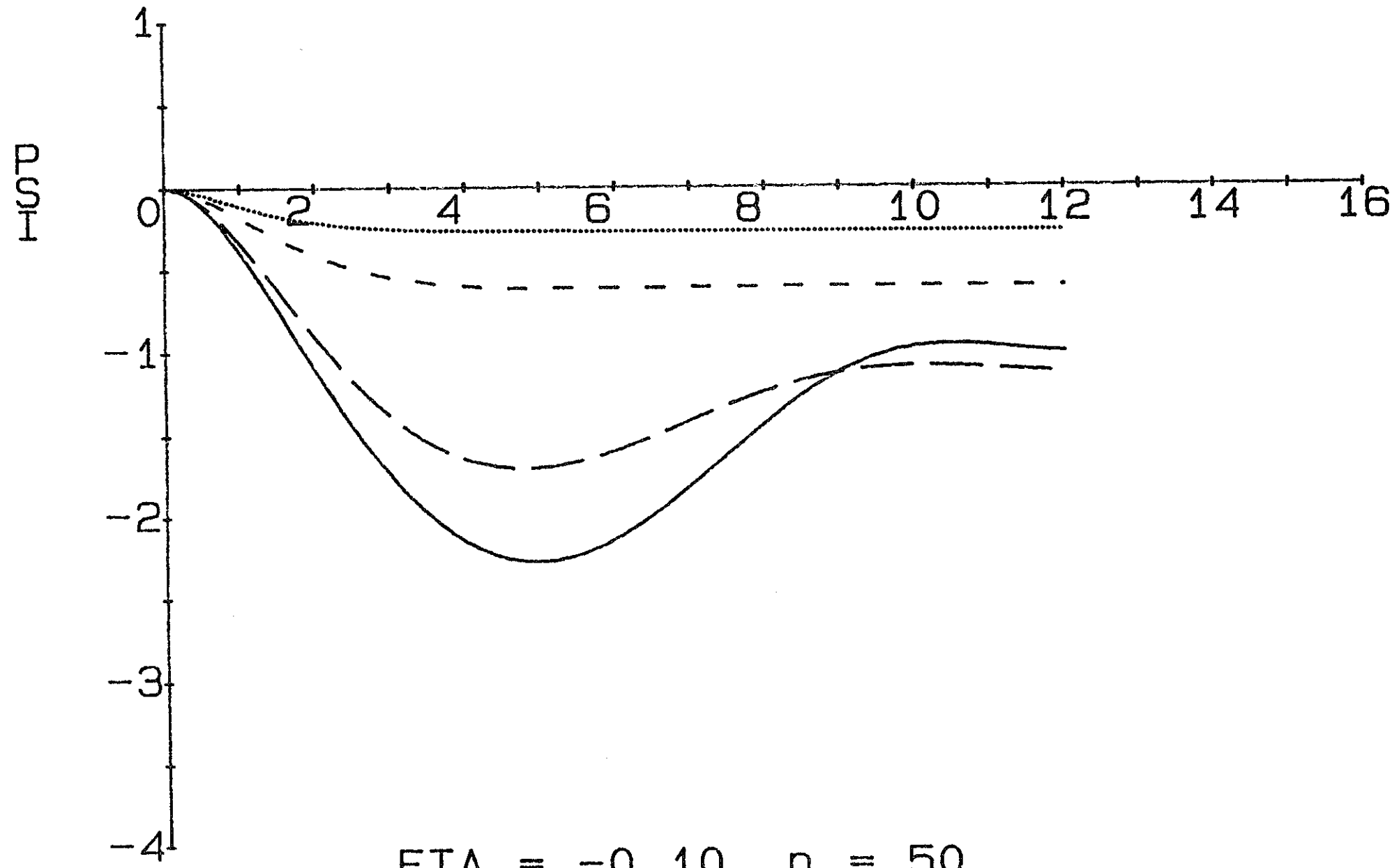


Figure 3

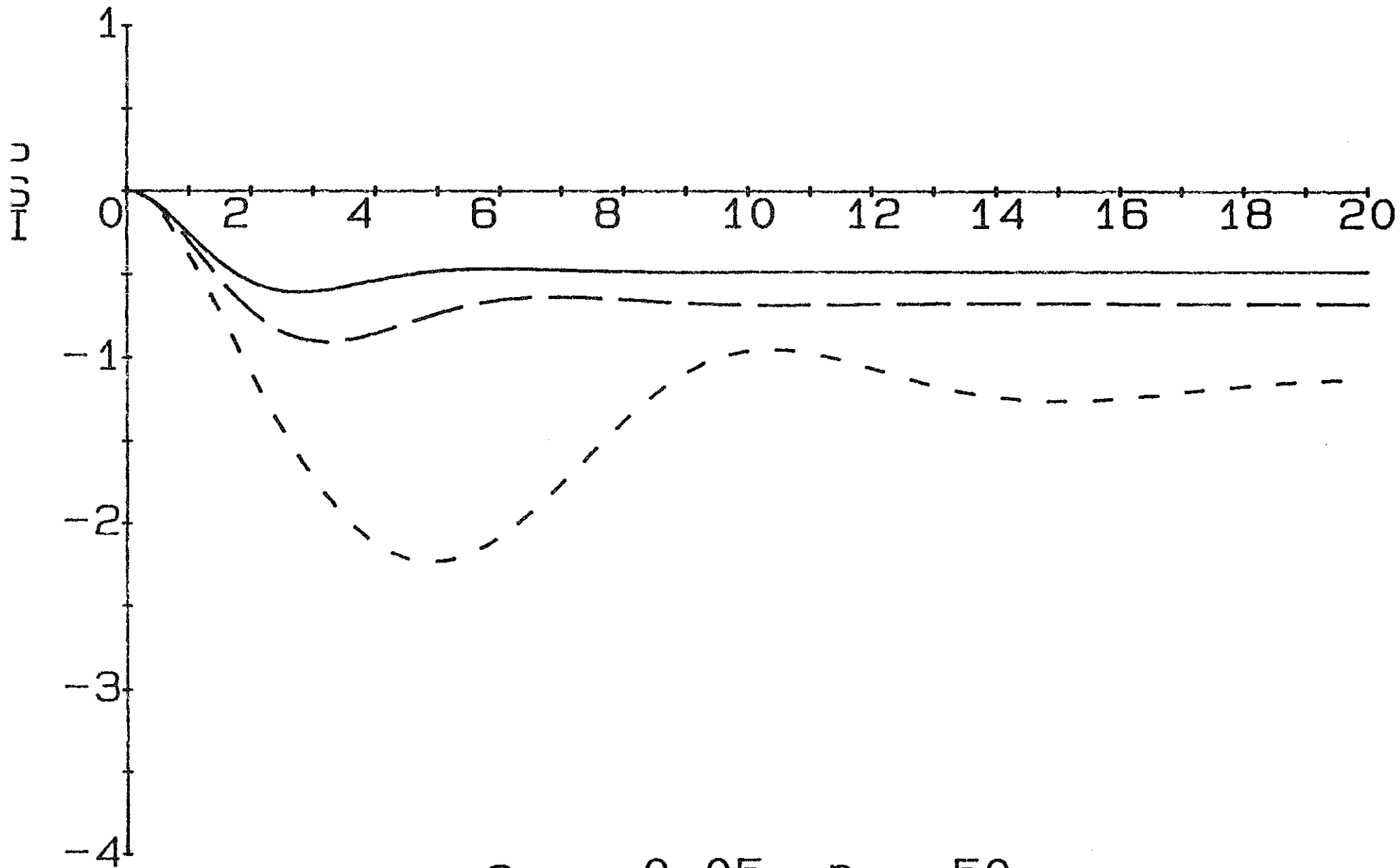


Figure 4

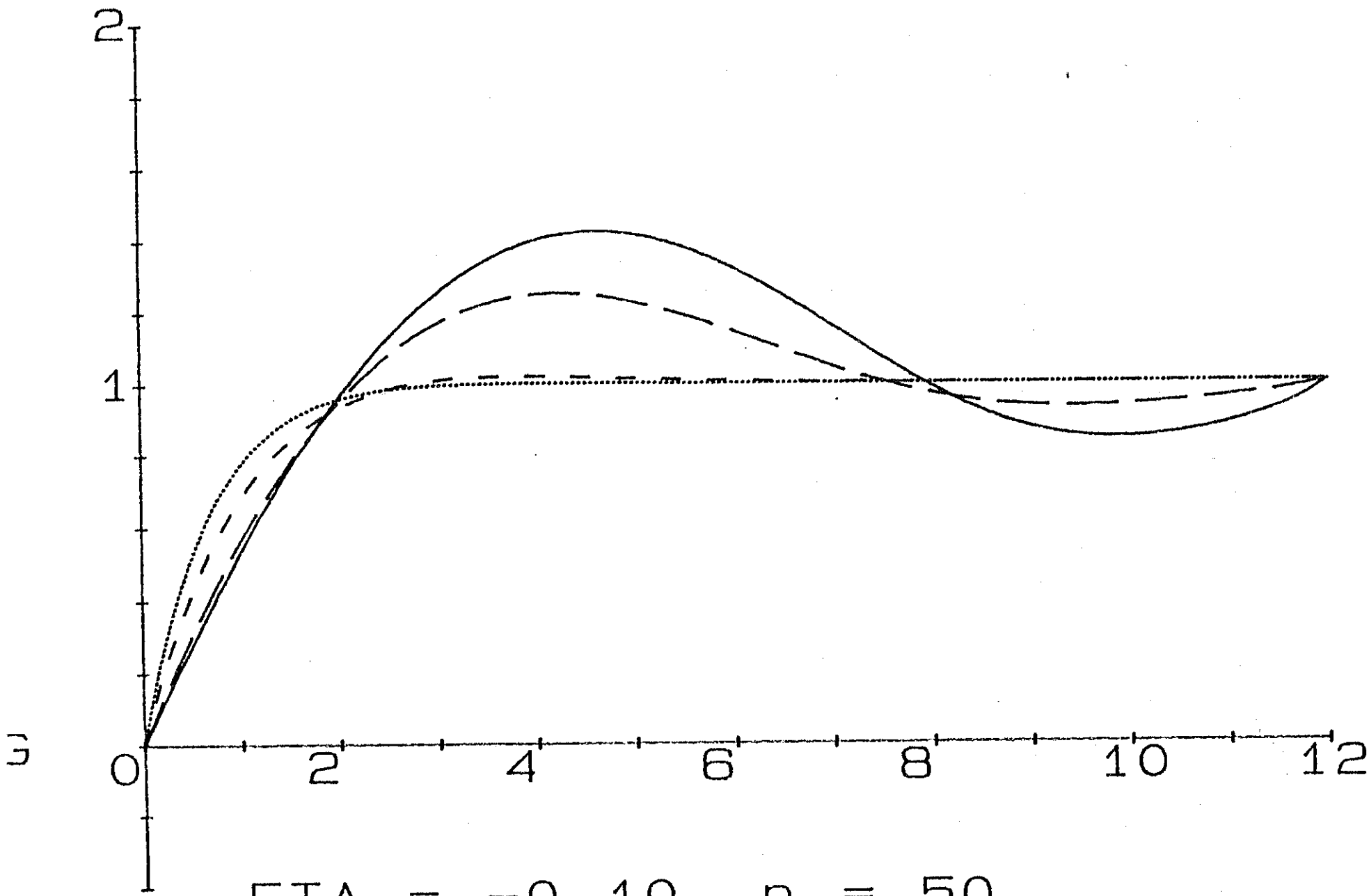


Figure 5

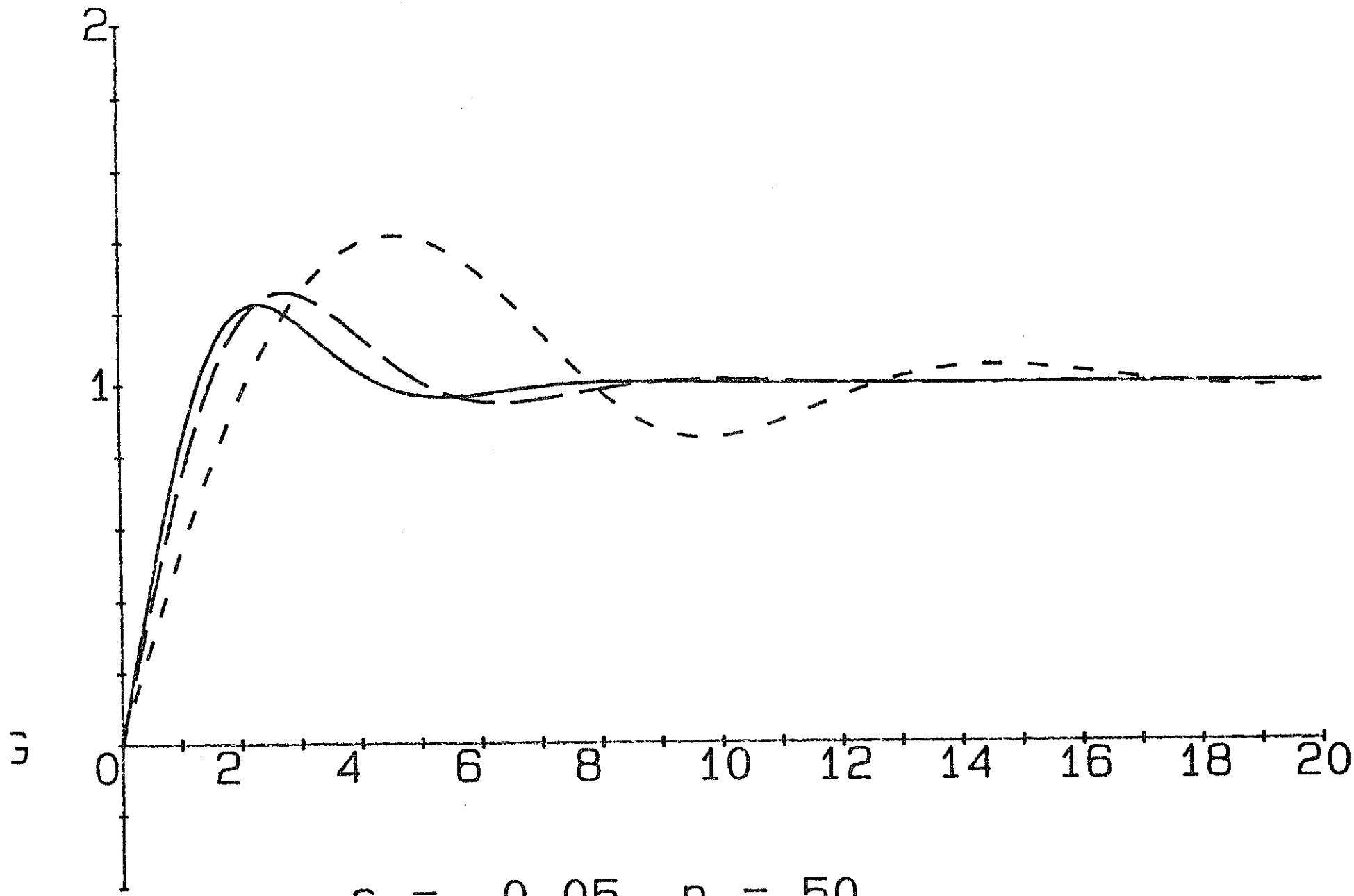


Figure 6

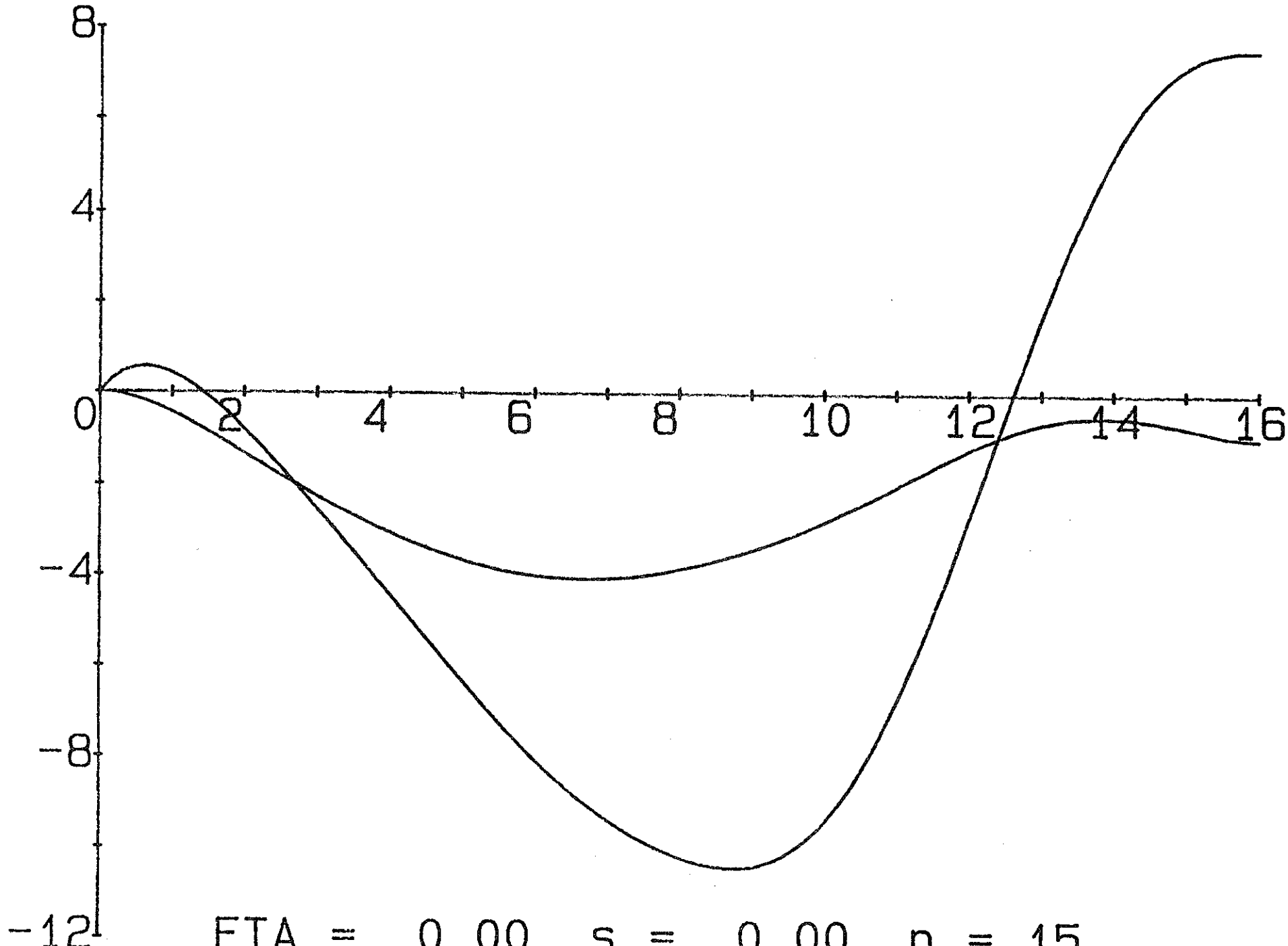


Figure 7

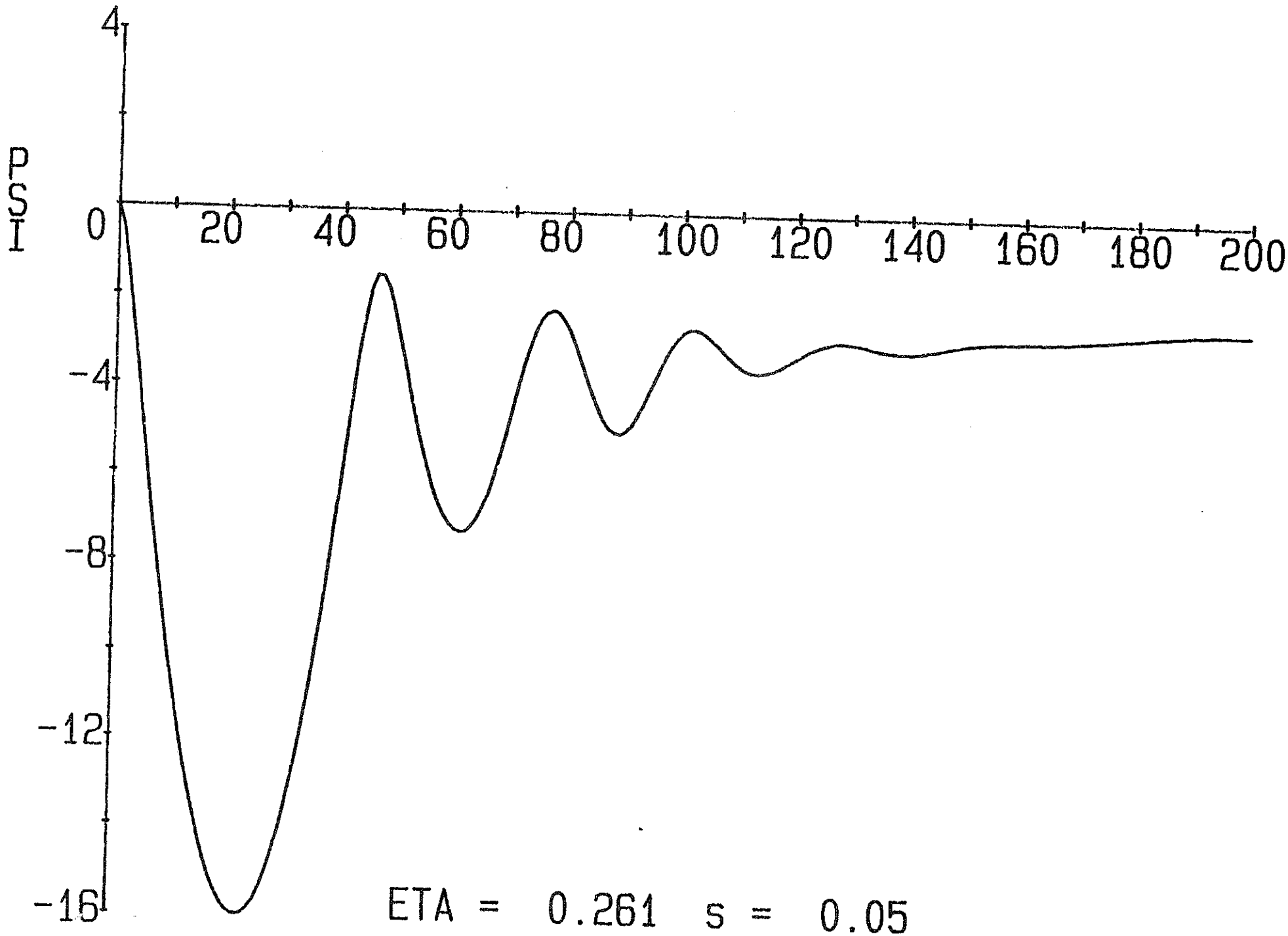


Figure 8